Isotopic effects of nitrate photochemistry in snow: A field study at Dome C, Antarctica

T. A. Berhanu[1,*], J. Savarino[1], J. Erbland[1], W. C. Vicars[1,¥], S. Preunkert[1], and [3]J. F. Martins[3], M. S. Johnson[4]

[1]*Universite Grenoble Alpes, LGGE, F-38000 Grenoble, France*

[2]*CNRS, LGGE, F-38000 Grenoble, France*

[3]*LTHE, UMR 5564, UJF-Grenoble 1/CNRS-INSU/G-INP, Grenoble*

[4]*Copenhagen Center for Atmospheric Research, Department of Chemistry, University of Copenhagen, Universitetsparken 5, DK-2100 Copenhagen Ø, Denmark*

[*]*Currently at Physics Institute, Climate and Environmental Physics, University of Bern, CH-3012 Bern, Switzerland*

[¥]*Currently at Technical Services Program, Air Pollution Control Division, Colorado Department of Public Health and Environment, Denver, CO, USA*

Abstract

Stable isotope ratios of nitrate preserved in deep ice cores are expected to provide unique and valuable information regarding paleo-atmospheric processes. However, due to the post-depositional loss of nitrate in snow, this information may be erased or significantly modified by physical or photochemical processes before preservation in ice. We have investigated the role of solar UV photolysis in the post-depositional modification of nitrate mass and stable isotope ratios at Dome C, Antarctica during the austral summer of 2011/2012. Two 30 cm snow pits were filled with homogenized drifted snow from the vicinity of the base. One of these pits was covered with a

plexiglass plate that transmits solar UV radiation, while the other was covered with a different plexiglass plate having a low UV transmittance. Samples were then collected from each pit at a 2-5 cm depth resolution and a 10-day frequency. At the end of the season, a comparable nitrate mass loss was observed in both pits for the top-level samples (0-7 cm) attributed to mixing with the surrounding snow. After excluding samples impacted by the mixing process, we have derived an average apparent nitrogen isotopic fractionation ($^{15}\varepsilon_{app}$) of (- 67.8 ± 12 ‰) for the snow nitrate exposed to solar UV using the nitrate stable isotope ratios and concentration measurements. For the control samples in which solar UV was blocked, an apparent average $^{15}\varepsilon_{app}$ value of -12.0 ± 1.7 ‰ was derived. This difference strongly suggests that solar UV photolysis plays a dominant role in driving the isotopic fractionation of nitrate in snow. We have estimated a purely photolytic nitrogen isotopic fractionation ($^{15}\varepsilon_{photo}$) of -55.8 ‰ from the difference in the derived apparent isotopic fractionations of the two experimental fields, as both pits were exposed to similar physical processes except exposure to solar UV. This value is in close agreement with the $^{15}\varepsilon_{photo}$ value of (-47.9 ± 6.8 ‰) derived in a laboratory experiment simulated for Dome C conditions (Berhanu et al., 2014). We have also observed an insensitivity of $^{15}\varepsilon$ with depth in the snowpack under the given experimental setup. This is due to the uniform attenuation of incoming solar UV by snow, as $^{15}\varepsilon$ is strongly dependent on the spectral distribution of the incoming light flux. Together with earlier work, the results presented here represent a strong body of evidence that solar UV photolysis is the most relevant post-depositional process modifying the stable isotope ratios of snow nitrate at low accumulation sites where many deep ice cores are drilled. Nevertheless, modeling the loss of nitrate in snow is still required before a robust interpretation of ice core records can be provided.

Introduction

Nitrate (NO_3^-), the end-product of the oxidation of atmospheric nitrogen oxides (NO_x = NO + NO_2), is one of the most abundant ions present in polar ice and snow. Ice core nitrate mass and isotopic measurements have the potential to provide quantitative constraints on historic variations in atmospheric NO_x cycling and oxidative capacity (Legrand and Kirchner, 1990; Wolff, 1995). However, the interpretation of these paleo-records is problematic at most sites on the polar ice sheets, where post-depositional processes such as the desorption of nitrate species on snow grains, sublimation/condensation of water vapor and photolysis of nitrate have a major influence on the signal archived in firn and ice (Dibb et al., 1998; Honrath et al., 1999; Röthlisberger et al., 2002; Blunier et al., 2005; Frey et al., 2009; Wolff, 2013). While desorption is manifested by the physical release of HNO_3 from the snow-pack, photolysis involves bond breaking in NO_3^- and emission of the photoproducts, such as NO_x, HONO and the hydroxyl radical (OH), which can alter the oxidative capacity of the overlying atmosphere (Chen et al., 2001; Crawford et al., 2001; Domine and Shepson, 2002; Grannas et al., 2007; Meusinger et al., 2014).

The stable isotope ratios of nitrate ($\delta^{18}O$, $\Delta^{17}O$ and $\delta^{15}N$) are useful metrics used to constrain NO_x chemistry (Savarino et al., 2007; Morin et al., 2008; Hastings et al., 2009; Savarino et al., 2013; Vicars et al., 2013) and the post-depositional processing of nitrate in snow (Blunier et al., 2005; Frey et al., 2009; Erbland et al., 2013). Stable isotope ratios (R) ($n(^{18}O)/n(^{16}O)$, $n(^{17}O)/n(^{16}O)$ and $n(^{15}N)/n(^{14}N)$) are expressed as isotopic enrichments/depletion ($\delta^{18}O$, $\Delta^{17}O$ and $\delta^{15}N$) relative to a reference where $\delta = (R_{spl}/R_{ref}) - 1$, and R represents the elemental $^{17}O/^{16}O$, $^{18}O/^{16}O$, or $^{15}N/^{14}N$ ratio in the sample or reference material. The $\Delta^{17}O$ value is defined here using the linear relation $\Delta^{17}O = \delta^{17}O - 0.52 \times \delta^{18}O$. The reference used for oxygen

77 isotope analysis is Standard Mean Oceanic Water (SMOW) and the reference for
78 nitrogen is atmospheric N_2. For practical reasons, δ values are typically reported in
79 per mill (‰), as variations in isotopic ratios for natural samples occur within a very
80 narrow range.

81 In order to constrain post-depositional effects on the concentration and stable
82 isotope ratios of nitrate, it is necessary to have knowledge of the isotopic fractionation
83 values (expressed using $^{15}\varepsilon$, $^{18}\varepsilon$, ^{17}E, see Eq. 1 for definitions), which are unique for
84 each post-depositional process. Blunier and co-workers analyzed two surface ice
85 cores from Dome C, Antarctica and determined a nitrogen isotopic fractionation ($^{15}\varepsilon$)
86 of (- 54 ± 10) ‰ (Blunier et al., 2005). In an attempt to reproduce this field
87 observation in the laboratory, artificial snow was irradiated with UV light in the 200–
88 900 nm wavelength range and a $^{15}\varepsilon$ value of (- 11.7 ± 1.4) ‰ was determined. The
89 authors concluded that post-depositional modification must therefore result primarily
90 from sublimation of snow/desorption of nitric acid, with only a minor contribution
91 from photolysis. However, it was later confirmed that the light source used in this
92 laboratory study possessed a different spectral distribution compared to solar spectra
93 encountered in the field, and this may have had a confounding effect on the
94 interpretation of the results (Frey et al., 2009). This effect was shown experimentally
95 in a recent laboratory study (Berhanu et al., 2014; Meusinger et al., 2014) by
96 irradiating natural snow from Dome C using different UV-filters to match field
97 conditions. Accordingly, isotopic fractionations became less negative and approached
98 zero when irradiated with short wavelength UV-light and vice-versa due to the
99 different overlaps of nitrate isotopologue cross-sections with the incoming UV. The
100 $^{15}\varepsilon$ value of (-47.9 ± 6.8) ‰ derived for the experiment conducted using a 320 nm
101 filter (closer to Dome C solar irradiance conditions), was in good agreement with the

field observations of (-54 ± 10) ‰ (Blunier et al., 2005), (-50 ± 10) ‰ and (-71 ± 12) ‰ by Frey et al. (2009) at Dome C. A recent field study by Erbland and colleagues determined an average apparent $^{15}\varepsilon$ value of (- 59 ± 10) ‰ for the East Antarctic Plateau (Erbland et al., 2013).

A theoretical framework has been developed by Frey and colleagues in order to determine isotopic fractionations associated with photolysis (Frey et al., 2009). The authors used the Zero Point Energy-shift model (ΔZPE) (Yung and Miller, 1997), convoluted with solar spectrum measured during summer solstice at Dome C, and determined a $^{15}\varepsilon$ value of - 48 ‰, consistent with their field observations. However, photolytic isotopic fractionations based solely on the ZPE-shift model are affected by the limitations of the model, such as ignoring the change in shape and intensity of the absorption cross-sections during isotopic substitutions (Schmidt et al., 2011). In a recent study, a semi-empirical model was developed that is based on the ZPE-shift model but addresses some of the limitations mentioned above (Berhanu et al., 2014). This model enabled better estimation of the absorption cross-sections of nitrate isotopologues, which can be interpolated to a temperature of interest, thus providing a better estimate for isotopic fractionations under field conditions.

The currently existing field studies (Blunier et al., 2005; Frey et al., 2009; Erbland et al., 2013) derived apparent isotopic fractionations (denoted $^{15}\varepsilon_{app}$, $^{18}\varepsilon_{app}$ and $^{17}E_{app}$), that incorporate not only the isotopic effects of photolysis but also other processes with the potential to induce isotopic fractionation (desorption, re-oxidation and surface deposition). In addition, the isotopic fractionations obtained in the existing field studies cover a wide range of $^{15}\varepsilon$ values (- 40 ‰ to - 74.3 ‰) (Erbland et al., 2013). Therefore, further experimental and modeling studies are required to

126 constrain the effects of photolysis on stable isotope ratios of nitrate in snow and to
127 advance the interpretation of these measurements in snow and ice.

128 We have performed a field study at Concordia (Dome C), Antarctica (75°06' S
129 and 123°19' E) during the Antarctic summer of 2011/2012. The effect of UV-
130 photolysis on snow nitrate and its associated effects on nitrate's stable isotopic
131 composition were investigated. We have employed an isolation technique to produce
132 UV-exposed and limited UV-exposed samples in order to understand the role of
133 photolysis in the post-depositional processing of snow nitrate. To the best of our
134 knowledge, this is the first field study that has employed an isolation strategy to
135 constrain specifically nitrate mass loss and the isotopic fractionation induced by
136 photolysis from solar UV radiation.

137 ## 2. Methods

138 ### 2.1. Experimental design

139 Wind-blown snow (i.e., drifted snow) was collected at Dome C on 02
140 December 2011 and physically homogenized in the field. This drifted snow possessed
141 a high nitrate concentration (≈1450 ppb), which ensured levels adequate for isotopic
142 analysis. Two snow pits of 1 m × 2 m surface area and 30 cm depth were excavated
143 within close proximity (~10 m) and filled with the drifted homogenized snow. A
144 rectangular wooden frame was used to mark each surface level at a fixed position
145 (i.e., depth = 0 cm). Hence, any additional windblown snow accumulating above this
146 wooden mark could be removed on a weekly or as needed basis. The pits were
147 covered with plexiglass plates of different UV transmittances (Figure 1), one having
148 only minor transmittance (10-15 %) below 380 nm, and the other allowing most of the
149 solar UV-radiation in the 290-380 nm range. Transmittance was measured as a ratio
150 between incoming solar light below the plexi-plate to light on top of the plate. Note

that sometimes light reflected back by the snow might lead to transmittance greater than one. For simplicity, the samples exposed to UV will be referred to as "UV" samples, while those collected from the other pit, which is expected to be unaffected by UV-driven photolysis, will be referred to as "control" samples. Note that other non-UV light associated effects are expected to affect both pits equally (e.g., the disturbance of outgoing long-wave radiation caused by the plates). Equally, it should be realized that a complete protection from UV radiations in the field is impossible due to scattering of light by the snow, high solar zenithal angles (min at solstice 51.6 °) and imperfection of the UV-cutting by the plexiglass. Such interferences are too complex to quantify but are mainly limited to the first cm of snow. The choice of the plexi-plates transmittance was based on the UV absorption cross-section of nitrate. Nitrate has UV absorption peaks around 200 nm and 305 nm, with the former being 3 orders of magnitude stronger than the latter (Mack and Bolton, 1999). However, light at the wavelengths of the strong 200 nm band is cut off because of the presence of the stratospheric ozone layer (Figure 2) and does not reach Earth's surface. The control plexi-plate blocks the secondary absorption band in contrast to the UV plexi-plates, which allow this band to reach the snow beneath. The plexiglass plates were placed on a metallic frame 20 cm above the snow surface, which is expected to be an optimum height because it minimizes both the warming effect on the snow beneath and the trapping of emitted NOx photoproducts. Placing the plates at a higher level could increase the possibility of snow deposition at the sides; furthermore, at higher solar zenith angles there may be solar UV radiation reaching the control plates. In contrast, vertical plates were not placed at the sides to avoid trapping drifted snow.

2.2. Sampling and concentration measurements

175 Sampling was conducted every 10 days from 2 December 2011 to 30 January
176 2012 at a 2-5 cm depth resolution and to a depth of 30 cm. Samples were collected
177 less frequently at depths below the homogenized snow (i.e., down to 50 cm). The
178 individual sampling events are indicated using numbers 0-6, with the numbers
179 increasing from the beginning to the end of the season. Below 50 cm, the photolysis
180 of nitrate becomes negligible, as demonstrated by the light transmission measured at
181 Dome C (France et al., 2011). The detailed sampling dates are given in Table 1.
182 Sampling was usually conducted in the morning between 9 - 12 local time, and with
183 few occasions one pit in the morning and another in the afternoon. During sampling
184 the plexi plates were removed so that both pits were exposed to direct solar UV for a
185 short period of time (usually less than an hour). For each sample, a snow mass of 0.3
186 – 0.6 kg was collected, placed into a two-liter (Whirl-Pack^{TM}) bag, and stored frozen
187 (note that in a few cases, a larger amount of snow, up to 1 kg was collected). The
188 vertical pipes created during sampling were backfilled using natural snow from
189 nearby, with a different nitrate amount and isotopic signature than the experimental
190 snow. A mark was left on the wooden frame after each sampling to record the place
191 where sampling was conducted. A gap of 10 cm was left between consecutive
192 samplings to ensure that subsequent samplings were not modified by previous
193 samplings. The samples were later melted at room temperature for nitrate
194 concentration measurement and preconcentration. The concentration of nitrate in each
195 sample was determined in a warm laboratory at the Dome C station using a
196 continuous flow analysis method. This is a fast technique used in previous studies by
197 our group at Dome C, with a precision of < 3 % and a detection limit of 5 ng g^{-1} (Frey
198 et al., 2009; Erbland et al., 2013). In this study, we have determined a precision of
199 about 5 % based on replicate standard measurements. Most of the melted snow

sample volume was preconcentrated using an anion exchange resin AG 1-X8 (Bio-Rad 200-400 mesh chloride form) to trap NO_3^- for isotopic analysis. This step is essential to ensure that enough samples are available for replicate measurements. The nitrate trapped in the resin was eluted with the addition of 5 × 2 ml 1M NaCl solution (Frey et al., 2009; Erbland et al., 2013). The samples were stored in plastic tubes in the dark and shipped frozen to Grenoble, France for isotopic analysis. We have also collected surface snow samples along with the snow pit sampling in the immediate vicinity in order to follow possible mixing of the surrounding snow with the snow pits. The analysis of these samples was conducted in a similar fashion as for the snow pit samples.

2.3. Isotopic analysis

The oxygen and nitrogen isotopic composition of nitrate was determined using the bacterial denitrifier method (Sigman et al., 2001; Casciotti et al., 2002; Kaiser et al., 2007; Morin et al., 2008) as modified by Kaiser et al. (2007) and Morin et al. (2009). Briefly, a culture of the denitrifying bacteria (Pseudomonas aureofaciens) was concentrated 8 times by centrifugation following a 5-7 day growth period. 2 mL of the bacterial culture were then transferred to a 20 mL glass vial, which was sealed airtight with a PTFE septum. The vials were then degassed for 3 hours using a helium flow (Air Liquide, 99.999%). 100 nmol of each preconcentrated nitrate sample was then injected into these vials using an automated system (Gilson Liquid Handler 215). After an overnight incubation, which allows for complete conversion of NO_3^- to N_2O (Sigman et al., 2001), 0.5 mL of 1 M NaOH was added to each vial to inactivate the bacterial cells. The N_2O in the sample vial headspace was then flushed with purified helium (99.999%), cryogenically trapped before transferred into a gold tube at 900 °C, where it was decomposed to O_2 and N_2 (Cliff and Thiemens, 1994; Kaiser et al.,

2007), which was separated by a GC column and passed into a MAT253 IRMS (Thermo Scientific) to determine the stable oxygen and nitrogen isotope ratios (Morin et al., 2009).

To correct for isotopic effects associated with sample analysis, we have included certified standards of USGS 32, USGS 34, and USGS 35 (Michalski et al., 2002; Bohlke et al., 2003), which were subjected to a treatment identical to the samples and prepared in the same matrix (1M NaCl solution prepared using Dome C water in order to match the oxygen isotopic composition of local water) (Werner and Brand, 2001; Morin et al., 2009). We have determined the overall accuracy of the method as the standard deviation of the residuals derived from the linear regression between the measured and expected values of the reference materials (Morin et al., 2009). For the samples analyzed in this study, the associated overall accuracies are 2.0 ‰, 0.4 ‰ and 0.6 ‰ for $\delta^{18}O$, $\Delta^{17}O$ and $\delta^{15}N$ respectively.

2.4. Data reduction

In order to quantify the effect of photolysis on the stable isotope ratios of snow nitrate, we have calculated apparent isotopic fractionations (isotopic fractionations derived for field samples irrespective of the process inducing fractionation) for O and N isotopes ($^{15}\varepsilon_{app}$, $^{18}\varepsilon_{app}$, and $^{17}E_{app}$ for $\delta^{15}N$, $\delta^{18}O$ and $\Delta^{17}O$ of nitrate, respectively) assuming an open system, where NO_x emitted upon the photolysis of nitrate will be removed as soon as it is formed and nitrate at depth is considered irreversibly lost (in contrast to the "skin layer" snow, which receives the deposition of re-oxidation products), and adopting the linear relation used in previous studies (Blunier et al., 2005; Erbland et al., 2013):

$$\ln(d+1) = e\ln(f) + \ln(d_0+1) \quad (1)$$

where f is the nitrate fraction remaining in snow, defined as the ratio of the final nitrate concentration (C) and the initial nitrate concentration (C_0) in the snow ($f = C/C_0$). δ_0 and δ are the isotope ratio values for the initial and final snow, respectively. Due to a hiatus in preparing the standards for each batch of analysis (an offset was observed between batches but not within a batch), the use of the initial concentration of the homogenized snow as the starting point was not possible. Instead C_0 was calculated using the average nitrate concentration measured at 25-30 cm depth, assuming there is no change in the amount of nitrate at this depth due to insufficient light penetration and short duration of experiment. The slope of the $\ln(\delta+1)$ versus $\ln(f)$ plot is the isotopic fractionation ε (note that $\varepsilon = (\alpha-1)$), where α is the fractionation factor.

Isotopic fractionation due to photolysis (denoted $^{15}\varepsilon_{photo}$) has also been determined in this study using the Zero Point Energy shift-model (ΔZPE) and the light transmittance of plexi-plates, as described in Frey et al. (2009). According to this model, during isotopic substitution, the ZPE of the heavier isotopologue is reduced, leading to a small blue shift in the absorption spectrum of the heavier isotopologue relative to the lighter one (Figure 2). Hence, from a light isotopologue with a measured absorption cross-section ($^{14}NO_3^-$), it is possible to derive the absorption-cross section of the heavier isotopologue ($^{15}NO_3^-$) (Yung and Miller, 1997; Miller, 2000). Isotopic fractionations (ε) were determined using the following equation:

$$\varepsilon = \frac{J'}{J} - 1 \qquad (2)$$

where J' and J are the photolytic rate constants of the heavier and lighter isotopologues, respectively, defined mathematically as:

$$J = \int \phi(\lambda,T)\sigma(\lambda,T)I(\lambda,\theta,z)d\lambda \qquad (3a)$$

$$J' = \int \phi(\lambda,T)\sigma'(\lambda,T)I(\lambda,\theta,z)d\lambda \qquad (3b)$$

where σ and σ' are the absorption cross-sections of the light and heavy isotopologues respectively. $\phi(\lambda)$ is the quantum yield and I is the actinic flux for the given wavelength ranges, which depends on the solar zenith angle (θ) and snow depth (z). Note that if $\phi(\lambda)$ is assumed to be independent of wavelength and is the same both for $^{14}NO_3^-$ and $^{15}NO_3^-$, then there is no need to know its value in order to determine the isotopic fractionation value. In this study, we have applied this principle and derived isotopic fractionations for the UV-exposed pit in the presence of the plexi-plates for field conditions.

We have also investigated the depth dependence of the isotopic fractionation using the concentration and isotope ratio profiles of nitrate in the experimental snow pits. Accordingly, samples from the same depths from the 7 sampling events were stacked together, and isotopic fractionations were determined from the measured nitrate concentration and $\delta^{15}N$ applying the Rayleigh plot approximation. Sampling at exactly the same depth during each collection was not possible under field conditions; therefore, the nitrate concentration and $\delta^{15}N$ values obtained for at least 4 different samples that were expected to be at the same depth, were used to derive the isotopic fractionation values. In a few cases, samples within a 1 cm depth range were averaged together to derive $^{15}\varepsilon$.

2.5. Experimental precautions

It is important to present the precautions taken in this study to minimize possible artifacts. The two experimental fields were open to the atmosphere despite the presence of the plexi-plates. Therefore, while the deposition of snow/nitrate was prevented at the top of the experimental fields, drifted snow could still have been deposited at the surface of the pits, as the sides were not closed, in addition to dry

298 deposition of gaseous HNO_3. In order to minimize the effect from drifted snow, we
299 mounted a wooden frame at the sides of the snow pits so that it was possible to
300 establish a reference surface level (depth = 0 cm), and the snow present above this
301 frame was carefully removed as needed. In addition, in order to avoid
302 absorption/reflection of solar UV by windblown snow deposited on top of the plexi-
303 plates, we cleaned the plates at least once a week. However, during strong winds and
304 bad weather, it was impossible to precisely maintain the reference frame location. The
305 lack of homogeneity within and between fields and possible dry deposition are
306 unavoidable sources of mixing and noise in the data obtained from this experiment,
307 especially for the first few centimeters of the pits.

308 **3. RESULTS**

309 **3.1. Concentration profiles**

310 Figure 3 shows the fraction of nitrate remaining in the snow for each field and
311 for each sampling event at 0, 2, 4 and 6 × 10 days (Note that only samples from even
312 numbered sampling batches are chosen for visual reasons as showing the entire data
313 would clutter the figures. The actual nitrate concentrations and fraction remaining for
314 the entire sampling events are shown in Figure 1 and Figure 2 of the supplementary
315 materials). Accordingly, at the beginning of the experiment (UV #0 and control #0, t
316 = 0), the concentration of nitrate was uniform with depth ($f \approx 1$). This corresponds to
317 an average nitrate concentration of (1431 ± 46.8) ng g^{-1} and (1478 ± 34.5) ng g^{-1} down
318 to a 30 cm depth for the control and UV pits, respectively.

319 For control #2, f is about 0.75 in the top 5 cm, but the profile stabilized below
320 10 cm, with $f \approx 1$. A significant nitrate change was observed for the controls #4 and
321 #6 when compared to controls #0 and #2, with f reaching 0.15 - 0.25 in the top 4 cm,
322 but higher f values ($f > 0.8$) were observed below 5 cm. The maximum nitrate change

($f < 0.3$) was observed at the surface. It is important to note that the change observed in the first top cm is not necessarily the result of a mass loss but could also result from mixing with surrounding snow with a lower nitrate concentration than the experimental snow, resulting in an apparent mass loss.

In contrast, samples from the pit exposed to UV radiation showed a decrease in nitrate mass up to a depth of 20 cm. For UV #2, a nitrate change of $f \approx 0.5$ was observed at the surface. But at lower depths, below 3 cm, only minor changes were observed ($f > 8$). The maximum nitrate change, with f reaching 0.2, was observed for UV #4 and UV #6. The decrease continued until a depth of 7 cm where f reached 0.4. Further minor decrease ($f > 0.75$) was observed up to a depth of 20 cm, and the decrease of nitrate ceased below 25 cm.

In general, the decrease of nitrate in the top 7 cm (grey shaded region) was comparable for both the control and UV samples (a further indication of a possible mixing process); however, the amount of nitrate mass decrease was different in each pit depending on depth and collection date.

For the surface snow samples, we have observed nitrate concentrations as high as 1500 ng g^{-1} in mid-December that decrease to 400 ng g^{-1} at the end of January (Figure 4). This concentration profile sometimes matches the concentration of nitrate measured at a depth of 0-2 cm in the snow pits, indicating a possible mixing/substitution by the surrounding snow.

3.2. Isotopic Analysis

Figure 5 shows the $\delta^{15}N$ profiles of the two pits for samples #0, #2, #4, and #6 (the $\delta^{15}N$ values for the duration of the sampling season are shown in Figure 3 of the supplementary materials). Controls #0 and #2 showed fairly uniform $\delta^{15}N$, with values ranging between -10 ‰ and 0 ‰. However, controls #4 and control #6

exhibited enrichment in $\delta^{15}N$ up to +15 ‰ for the surface samples (0-2 cm depth) extending to a depth of about 7 cm, and subtle changes below a 10 cm depth.

In the case of the UV samples, only UV #0 showed stability upto a 30 cm depth, with $\delta^{15}N$ values ranging between -6 ‰ and -8 ‰. For the top 5 cm samples of UV #2, the $\delta^{15}N$ values showed an increasing pattern, with a maximum value at the surface (+12 ‰), and a stable $\delta^{15}N$ profile below 5 cm depth. Comparable $\delta^{15}N$ values and similar profiles were observed for UV #4 and UV #6, with a maximum $\delta^{15}N$ value of +35 ‰ at a depth of 2-4 cm. However, a decrease in $\delta^{15}N$ towards the surface was observed, and this profile is not consistent for all samples. All of the UV samples (excluding UV #0) have decreasing $\delta^{15}N$ values from their respective maximum value to about +8 ‰ to +14 ‰ near the snow surface (ca. 0 - 2 cm), irrespective of the sampling time. Meanwhile, this pattern is also apparent for control #4 and control #6.

For the surrounding surface snow samples, $\delta^{15}N$ values varying between -10 ‰ and +40 ‰ were measured on different days (Figure 6). However, no trend was observed in the $\delta^{15}N$ values over time. These values are sometimes similar to what is measured at the surface of the two pits, consequently we believe that the first 7 cm in both pits weas subjected to mixing with the surrounding snow.

Figure 7 shows the $\delta^{18}O$ values obtained for both the control and UV samples, which ranged from 52 ‰ to 68 ‰. It is difficult to detect a consistent trend between $\delta^{18}O$ and depth or sampling period for either the control or UV samples in this data set.

Similar to the $\delta^{18}O$ observations, the measured $\Delta^{17}O$ values also exhibited no significant trend, with values ranging between 26 ‰ and 30 ‰ obtained for both pits (Figure 8). However, comparing the control and UV samples, more variability is observed in the $\Delta^{17}O$ values of the UV samples.

In general, when comparing the stable oxygen isotope ratios of the control and UV samples, it is difficult to identify any pattern or significant difference between the two sets with respect to sampling event (Figures 7 and 8). However, a significant difference is observed between the two pits (control and UV) for δ^{15}N. The measured δ^{15}N values are the main results, used in this study to understand the role of photolysis in the post-depositional processing of snow nitrate.

4. DISCUSSION

4.1. Processes possibly acting on the top 0-7 cm depth

As this experimental study is based on the comparison of results obtained from two pits filled with a common drifted snow, our first priority was to ensure that the two pits were as identical as possible at the beginning of the study, and minimize or possibly prevent non-photolytic process. Figures 3 and 5 show a uniform nitrate mass fraction left in the snow ($f \approx 1$) as well as a fairly stable δ^{15}N (-6 ‰ to -8 ‰) profile up to a 30 cm depth for both UV #0 and control #0. This observation indicates that the snow was well homogenized and both pits had comparable initial nitrate concentrations and isotopic compositions. However, a significant change of nitrate and enrichment in δ^{15}N was observed on the top 0 – 7 cm depth (grey shaded area) after consecutive sampling events according to Figures 3 and 5, even in the absence of direct solar UV light. This observation, together with the decreasing δ^{15}N pattern observed near the surface layers with opposite direction to the expected enrichment at similar depths, implies that additional processes besides photolysis may be involved at these depths. Based on this observation, we have divided the two pits into two regions: the top 0-7 cm samples, where photolysis, mixing and additional processes are expected to act strongly, and samples collected at a 7-30 cm depth, where the effect of these additional processes is minor and photolysis is the dominant process

inducing nitrate mass loss and isotopic fractionation. We have discussed below the possible causes for nitrate mass loss in the top 7 cm, which is summarized in Figure 9.

Dome C generally experiences moderate wind speeds, with an average value of 2.9 m s^{-1} throughout the 1984-2003 meteorological record (Aristidi et al., 2005; Zhou et al., 2009), but even in this range of wind speeds deposition and erosion of snow is possible at the surface. Even though the new snow deposited above the reference surface level was removed 1-2 times per week, the snow might have already been mixed with the underlying surface layer and manual removal may have disturbed or mixed the two layers, even with extremely careful handling. Furthermore, erosion and replacement are also expected to take place during strong wind events. In addition, the drifted snow on the surface of the two pits was not always evenly deposited; more snow was often deposited on one pit relative to the other, and the deposition was not homogeneous even within a single pit. This variability could have led to changes in the surface reference level between each sampling event and may have thus introduced additional artifacts in these samples.

Snowfall was not observed during the sampling period; therefore, wet deposition of nitrate via snowfall is excluded. However, dry deposition of HNO_3 is still possible even with the plates in place. An interesting observation was the convergence in both the nitrate concentration and $\delta^{15}N$ values among the surface snow samples from the different batches. For the surface snow pit samples, both of these values converge on $f \approx 0.3$ and $\delta^{15}N \approx +10$ to $+14$ ‰ (mainly in the UV #2-6 and control #4-6 samples), as can be seen in Figures 3 and 5. These values contradict expectations based on the concentration and $\delta^{15}N$ profile observed below 7 cm. This implies that there might be snow deposition or mixing at the surface of the pits with snow with lower nitrate concentration (Figure 4) and a different isotopic composition

($\delta^{15}N \approx +10$ to $+14$), giving a false impression of mass loss. As these measured values are sometimes in agreement with the surface snow measurements from a similar time period (Figure 6), the presence of deposition is inevitable. For example, on 10 Jan 2012 we observed drifted snow on both snow pits (refer to the field logbook in supplementary materials) with similar nitrate concentration and stable isotope ratios as the nearby surface snow measurement. However such events were sporadic and apparently depended on meteorological conditions.

Another important process to consider is the re-deposition of nitrate via dry deposition. NO_x photoproducts can be locally reoxidized to reform nitrate and eventually re-deposited on the snow surface. It should also be noted that desorption may have taken place from the surface of both of the pits, which could be enhanced by the plexi-plates trapping heat and warming the top layers. This effect should be manifested in both pits and should affect mainly the top few cm of the snow. The pits exhibited comparable loss of nitrate mass in the top 7 cm, but the $\delta^{15}N$ values were significantly different for the two pits, with minimum $\delta^{15}N$ values of -15.0 ‰ and -36.0 ‰ for the control and UV pit samples, respectively. However, the more highly negative isotopic fractionation observed for the UV samples was probably due to the dominance of photolysis over the non-photolytic processes present in both pits.

Another possible reason for the observed nitrate mass change and resulting isotopic effect could be photolysis in both pits. The plexi-plate over the control pit excluded the majority of UV light at wavelengths shorter than 380 nm. However, 10-20 % of the incoming solar UV in the range 300 - 310 nm is transmitted through this plate (Figure 1), thus resulting in a spectral distribution in the control pit that overlaps with the nitrate UV absorption band. Additionally, at higher solar zenith angles, there

might be direct solar UV impeding upon the sides of the plexi-plates leading to photolysis.

In general, there are multiple processes (Figure 9) that can alter the concentration and isotopic composition of nitrate in the top 7 cm of snow. Identifying these processes and quantifying them is beyond the scope of this study. Hence, in this manuscript the samples from 7-30 cm depth range will be mainly considered with few exceptions when results are consistent with a unidirectional process.

4.2. Isotopic fractionations

Due to an insignificant change in nitrate mass and isotopic composition, the linear fits for samples #0 and #1 from both pits were only weakly correlated, and are not discussed. Better correlations were observed for samples collected late in the season.

4.1.1. The Nitrogen isotopic fractions: $^{15}\varepsilon$

The calculated nitrogen isotopic fractionation values (i.e., the slopes of the Rayleigh plots, correlation coefficients and p-values) for samples between 7 and 30 cm depth in the control and UV pits are given in Table 2. Figure 10 shows the $^{15}\varepsilon_{app}$ values determined for the control and UV samples collected below 7 cm. Accordingly, the control samples possessed nearly constant and small negative apparent isotopic fractionation values between (-7.4 ± 2.3) ‰ and (-15 ± 0.9) ‰. In contrast, the UV samples shown in Fig. 10 exhibited higher negative apparent nitrogen isotopic fractionations ranging from (-18.0 ± 7.3) ‰ to (-58.3 ± 20.0) ‰, which became progressively more negative over time. According to this figure, it seems that either $^{15}\varepsilon$ evolves over time (i.e., from collection event #2 to #6), which contradicts theory (Berhanu et al., 2014), or there is an artifact introduced by removing the samples collected in the top 7 cm, where relatively larger nitrate mass change and isotopic

fractionation was observed. An artifact due to removing all the samples at 0 – 7 cm depth is the most probable one considering removing the depth where the nitrate mass fraction left was minimal (about 80 % nitrate is lost) and enrichment in $\delta^{15}N$ was significant when compared to depths below 7 cm. An alternative approach is to use the nitrate $\delta^{15}N$ signal to identify data points that may be impacted by one or more of the processes explained above. Accordingly, the bending pattern in $\delta^{15}N$ observed for samples near the surface layers implies either the presence of another process, or contamination by windblown snow with a different isotopic composition. Therefore, we have excluded the samples from the surface level when the $\delta^{15}N$ begins to decrease instead of increasing to more positive values, and then recalculated the isotopic fractionations. Accordingly, only data points between 0 - 2 cm were excluded for sampling events UV#0 to UV#3. For later sampling events, UV#4 to UV#6, samples between 0 – 6 cm depth were not considered in the new calculation of isotopic fractionations. The exclusion of more data points in the case of later sampling events was probably due to the fact that the external processes had more time to play a role in the modification of the near surface snow. The plots made based on these corrections are also shown in Figure 10. $^{15}\varepsilon_{app}$ values ranging from -59.8 ‰ to -73.0 ‰ were obtained, irrespective of the sampling time. Therefore, the pattern observed under the first assumption (i.e., excluding all points in the top 7 cm) introduced an apparent evolution of $^{15}\varepsilon_{app}$ over time as an artifact of the analysis. The average apparent isotopic fractionation values derived using the second approach (-67.8 ± 12 ‰) are in excellent agreement with previous average apparent isotopic fractionations of (-60 ± 10 ‰) at Dome C (Frey et al., 2009) and (-59 ± 10 ‰) for the East Antarctic Plateau (Erbland et al., 2013) (Table 3). This data exclusion procedure based on $\delta^{15}N$ signal was applicable only to samples from sampling events between Control#4 and

497 Control#6 as samples from the first two (Control#2 and Control#3) showed no
498 deviation in $\delta^{15}N$ from the expected pattern (Figure 3) and we have calculated a $^{15}\varepsilon_{app}$
499 value of (- 12.0 ± 1.7 ‰). As shown in Table 2, the observed change in the calculated
500 $^{15}\varepsilon_{app}$ was minor.

501 Based on the significant difference between the $^{15}\varepsilon_{app}$ values of the control and
502 UV samples, it is clear that the more highly negative isotopic fractionation is
503 associated with solar UV photolysis. However, the small negative nitrogen isotopic
504 fractionation (an average of -12.3 ± 1.7 ‰) observed for the control samples may be
505 due to a combination of minor photolysis and sublimation/desorption (which is
506 present in the UV pit as well). Even if a comparable mass loss of nitrate was observed
507 in the top 7 cm of both pits, the $\delta^{15}N$ values are significantly different (Fig. 5). As the
508 absorption cross section of nitrate is limited at wavelengths shorter than 340 nm,
509 photodissociation of nitrate is not expected at wavelengths longer than 375 nm (i.e.,
510 the cut-off of the control plexi-plate). However, minor contributions from the average
511 15 % transmittance of the control plexi-plate and/or direct solar UV photolysis at high
512 solar zenith angles and UV light scattering by the snow could potentially have
513 resulted in some minor photolysis in the control pit, even if no systematic bias was
514 observed between edge and center samples. This implies that another process (e.g.,
515 sublimation of snow, desorption of nitrate) could possibly take place and produces a
516 significant nitrate mass change with only a minor change in isotopic composition. In a
517 recent study of post-depositional isotopic effects in snow nitrate, it was verified that
518 sublimation of snow leads to an overall ^{15}N isotopic fractionation close to zero (0.9 ±
519 1.5 ‰ at -30°C, a temperature relevant at Dome C), whereas natural snow is observed
520 with a highly negative fractionation ($^{15}\varepsilon_{app}$ = - 59 ± 10 ‰) (Erbland et al., 2013).
521 Therefore, a mixing of the evaporative and photolytic fractionation processes could

conceivably result in an isotopic fractionation on the order -12 ‰ in the control pit. In contrast, photolysis is the dominant process in the UV pit due to the presence of unobstructed solar UV, and we have determined highly negative isotopic fractionations ($^{15}\varepsilon$ = -67.8 ± 12.0 ‰). Considering the presence of multiple processes, we cannot consider the values derived from the UV pits to represent purely photolytic isotopic fractionation values, but rather apparent $^{15}\varepsilon_{app}$ values, impacted minimally by non-photolytic processes. Hence, the best estimate for purely photolytic isotopic fractionation ($^{15}\varepsilon_{photo}$) under the current experimental setup would be the difference between the apparent isotopic fractionations determined for the UV and control pits (-55.8 ‰), as both pits were exposed to identical physical processes except exposure to solar UV. This value is in good agreement with a recent laboratory study by Berhanu et al. (2014), who irradiated natural snow collected at Dome C using a UV lamp with a 320 nm filter (similar but not identical to field conditions), a $^{15}\varepsilon_{photo}$ of -47.9 ± 6.8 ‰ was reported (Berhanu et al., 2014). The slightly less negative $^{15}\varepsilon_{photo}$ value obtained for the laboratory experiment may be the result of an inability to fully reproduce the solar spectrum under laboratory conditions, in contrast to the field where the snow was exposed to natural solar UV.

We have also made a comparison between the isotopic fractionations obtained from the field study and a theoretical estimate made using the ΔZPE-shift model, as described in Frey et al. (2009) and recently modified by Berhanu et al. (2014). The newly modified model incorporates changes in width and amplitude, in addition to changes in the center wavelength, during isotopic substitution. By applying a 1 % width reduction factor and an amplitude increase of 1 %, in addition to a shift of +32.5 cm^{-1} in the center of the absorption cross section of $^{15}NO_3$ relative to $^{14}NO_3$, the authors derived an apparent $^{15}\varepsilon$ value of -55.1 ‰ under Dome C conditions (Berhanu

et al., 2014). Following this approach and considering the solar UV transmittance of the plexi-plates, as well as using the solar actinic flux measured at Dome C on 7 January 2012 at 2 P.M. local time (Ghislan Picard, personal communication), we have calculated a $^{15}\varepsilon_{photo}$ value of -52.6 ‰ for the UV exposed pit. This value is also in agreement with the $^{15}\varepsilon_{photo}$ obtained from the laboratory study, but higher than the value determined for the UV pit, implying that complications arise from multiple processes in the field study. However, we note that the difference between the UV and control experiments brings the apparent isotopic fractionation closer to the pure photolysis isotopic fraction value (- 67.8 ‰ to – 55.8 ‰).

4.1.2. Oxygen isotopic fractionations: $^{18}\varepsilon$ and ^{17}E

For the control pit samples, we have determined $^{18}\varepsilon$ values ranging from -2.1 ‰ to 3.9 ‰ with an average value of (0.2 ± 2.6) ‰. These low $^{18}\varepsilon$ values are due to an insignificant change in isotopic values. In contrast, the UV exposed snow samples have nearly stable $^{18}\varepsilon$ values ranging from 9.0 – 13.0 ‰ and an average value of (12.5 ± 6.7) ‰, in good agreement with previous measurements (Table 4).

The ^{17}E values for the control samples were not significantly different from zero, whereas the UV samples possessed ^{17}E values of 1.1 ‰ to 2.2 ‰ with an average ^{17}E value of (2.2 ± 1.4) ‰, in good agreement with previous studies (Table 4). This is probably due to the "cage effect", wherein the photoproducts resulting from the photolysis of nitrate immediately undergo isotopic exchange with the surrounding OH/water ($\Delta^{17}O \approx 0$) and reform secondary nitrate with $\Delta^{17}O$ values approaching zero (McCabe et al., 2005). However, compared to the variations observed in snow and ice below the photic zone (> 5 ‰) (Erbland et al., 2013; Sofen et al., 2014), changes of $\Delta^{17}O$ due to the cage effect (ca. 2 ‰) can be considered negligible. Another interesting observation is the greater scattering of the $\Delta^{17}O$

observed for the UV pit, clearly indicating that the cage effect phenomenon is initiated by UV radiation.

4.2. Depth dependence of isotopic fractionations

For the samples collected at a depth of 7-20 cm from all batches and then binned together according to depth, the derived isotopic fractionations at each depth are shown in Figure 11. We have calculated a nitrogen isotopic fractionation value ranging from -7.8 ‰ to -23.6 ‰ for the control samples in the 7-16 cm depth range. However, the UV samples exhibited more highly negative fractionations ranging from -52.2 ‰ to -65.9 ‰ with depth. The average $^{15}\varepsilon_{app}$ value of (-59.9 ± 24.7) ‰ derived for these samples is in good agreement with the average apparent isotopic fractionation of (- 67.9 ± 12.0) ‰ derived from the experimental UV-exposed pit. The large error bars in Figure 11 are due to the small sample size and the relatively large uncertainty in the depth measurement, as all the layers might not have been at exactly the same depth during each sampling event, which may have led to the mixing of layers. The depth could also have changed over the course of the study due to the compaction of the snow with time. The insensitivity of $^{15}\varepsilon_{app}$ with depth implies that, even if the number of photons decreases with depth in the snowpack, the spectrum of the solar actinic flux is not strongly altered, at least to the depth considered in this study. Berhanu et al. (2014) also observed a similar depth insensitivity of the nitrogen isotopic fractionations in their laboratory study, where snow from Dome C was irradiated with a UV lamp closely matching the solar irradiance encountered at Dome C. From their measurement of actinic flux with depth in a snow column, a uniform attenuation of incoming flux was observed, leading to almost constant $^{15}\varepsilon$ values with depth in the snow column. The insensitivity of $^{15}\varepsilon$ with depth is a useful feature for the analysis of δ^{15}N records obtained from deep ice cores used to understand past

atmospheric changes, simplifying the interpretation of the $\delta^{15}N$ records associated with solar UV-photolysis at different depths. Different modeling studies (such as the TRANSIT model (Erbland et al., 2015)) are currently attempting to use ice core $\delta^{15}N(NO_3^-)$ records to constrain historic variations in atmospheric oxidation capacity, changes in the ozone column, and solar variability.

The $^{18}\varepsilon$ and ^{17}E values derived with depth also have a very weak Rayleigh fitting at lower depth (below 10-15 cm), and are associated with large uncertainties. This is mainly due to the minor change in the oxygen isotopic signal, in stark contrast to the N isotopes, where relatively strong signals were obtained. Further studies will be required to better constrain the isotopic fractionations, especially for oxygen isotopes.

5. Conclusions

In this experimental study from Dome C, Antarctica we have investigated the effect of photolysis on the concentration and stable isotope ratios of nitrate in snow by comparing two identical snow pits, with one of the two exposed to solar UV. Using the combined concentration and $\delta^{15}N$ signals, we have determined an average $^{15}\varepsilon_{app}$ value of (-67.8 ±12) ‰ for UV-exposed samples collected at a 10-day frequency between 1 December 2011 and 30 January 2012. These values were fairly stable throughout the season and are in good agreement with previously determined isotopic fractionations at Dome C. These values are significantly different from the $^{15}\varepsilon_{app}$ values obtained for the control samples (-12.3 ± 1.7 ‰). Considering the fact that the two experimental pits were exposed to identical physical processes, the difference in their apparent isotopic fractionation (- 55.8 ‰) should be considered as the best estimate of isotopic fractionation due to photolysis.

When compared to the $^{15}\varepsilon_{photo}$ values of (-47.9 ± 6.8) ‰ obtained in a laboratory experiment by Berhanu et al. (2014), where the photolytic process was isolated, the measured values for the UV-exposed samples are slightly lower (i.e., more highly negative). This difference might be associated with experimental design, as the laboratory conditions do not exactly replicate the solar spectrum, even if better control is possible in terms of temperature stability, and product removal relative to the field experiment. Other confounding factors may include differences in the chemical domain of nitrate (Meusinger et al., 2014), or changes due to the temperature dependence of the nitrate absorption cross-section. It should also be noted that the field experiments show small influences due to non-photolytic processes such as desorption, deposition, and/or contamination by windblown snow.

We have also determined the depth dependence of the isotopic fractionations from the UV exposed snow pit samples that were binned together according to depth, and observed that the $^{15}\varepsilon_{app}$ values are nearly insensitive to depth. Despite the fact that the $^{15}\varepsilon_{app}$ values derived at different depths are associated with larger error bars, the observations are in good agreement with a previous laboratory study (Berhanu et al., 2014). In addition, previous studies did not show a strong change in spectral distribution of UV light as light propagates through the snow (Meusinger et al., 2014). Further study is necessary to validate such conclusions, for example via sampling different sites with same depth profiles and determining the isotopic fractionations.

It is important to reiterate some of the possible limitations of this experiment. Due to the unavoidable mechanical modification of the snow during the filling of the sample pits with wind-blown snow, the snow used in this study did not possess identical physical properties (grain size, density, compactness, optical properties, etc.) compared to the natural snowpack. This may have resulted in a modification of light

scattering within the snowpack. Additionally, the snow used in this study possessed a nitrate concentration more than an order of magnitude higher than what is normally measured in snow pits at Dome C, and this may have impacted nitrate chemistry in the experimental snow pits. However, to the best of our knowledge, our study is the first to attempt a replication of field constraints (natural shape and size, natural concentration and exposure, natural location of the nitrate in the snow grains, as well as meteorological conditions). Finally, we have not included some of the data points in the top layers of both pits due to possible complications due to multiple processes (mixing, sublimation, desorption, contamination, etc.). Hence, this procedure may have also introduced a small underestimation in our $^{15}\varepsilon_{app}$ values, and this should be kept in mind when using the values obtained in this study.

The results obtained here, together with results described previously in the literature (Frey et al., 2009; Erbland et al., 2013; Berhanu et al., 2014) represent a strong body of evidence that solar UV photolysis is the most relevant post-depositional process modifying stable isotope ratios of snow nitrate at low accumulation sites, where most deep ice cores are drilled.

Acknowledgement

The research leading to these results has received funding from the European Community's Seventh Framework Programme (FP7/2007-2013) under the grant agreement number 237890. LEFE-IMAGO, a scientific program of the Institut National des Sciences de l'Univers (INSU/CNRS), has also provided partial funding for this study. We would like to thank INSU for its financial support for lab experiments through its LEFE program. The Agence nationale de la recherche (ANR) is gratefully acknowledged for its financial support through the OPALE project (contract NT09-451281). The Institute Polaire Paul-Emile Victor (IPEV) supported the research and polar logistics through the program SUNITEDC No. 1011. This work has been partially supported by a grant from Labex OSUG@2020 (Investissements d'avenir – ANR10 LABX56. We would also like to thank Erwan Vince for his significant contribution in sample analysis.

References

Aristidi, E., Agabi, K., Azouit, M., Fossat, E., Vernin, J., Travouillon, T., Lawrence, J. S., Meyer, C., Storey, J. W. V., Halter, B., Roth, W. L., and Walden, V.: An analysis of temperatures and wind speeds above Dome C, Antarctica, Astron Astrophys, 430, 739-746, Doi 10.1051/0004-6361:20041876, 2005.

Berhanu, T. A., Meusinger, C., Erbland, J., Jost, R., Bhattacharya, S. K., Johnson, M. S., and Savarino, J.: Laboratory study of nitrate photolysis in Antarctic snow. II. Isotopic effects and wavelength dependence, J Chem Phys, 140, Artn 244306 Doi 10.1063/1.4882899, 2014.

Blunier, T., Floch, G. L., Jacobi, H. W., and Quansah, E.: Isotopic view on nitrate loss in Antarctic surface snow, Geophys Res Lett, 32, doi: 10.1029/2005gl023011 2005.

Bohlke, J. K., Mroczkowski, S. J., and Coplen, T. B.: Oxygen isotopes in nitrate: new reference materials for O-18 : O-17 : O-16 measurements and observations on nitrate-water equilibration, Rapid Commun Mass Sp, 17, 1835-1846, Doi 10.1002/Rcm.1123, 2003.

Casciotti, K. L., Sigman, D. M., Hastings, M. G., Bohlke, J. K., and Hilkert, A.: Measurement of the oxygen isotopic composition of nitrate in seawater and freshwater using the denitrifier method, Analytical Chemistry, 74, 4905-4912, Doi 10.1021/Ac020113w, 2002.

Chen, G., Davis, D., Crawford, J., Nowak, J. B., Eisele, F., Mauldin, R. L., Tanner, D., Buhr, M., Shetter, R., Lefer, B., Arimoto, R., Hogan, A., and Blake, D.: An investigation of South Pole HOx chemistry: Comparison of model results with ISCAT observations, Geophysical Research Letters, 28, 3633-3636, Doi 10.1029/2001gl013158, 2001.

719 Cliff, S. S., and Thiemens, M. H.: High-Precision Isotopic Determination of the O-
720 18/O-16 and O-17/O-16 Ratios in Nitrous-Oxide, Anal Chem, 66, 2791-2793, Doi
721 10.1021/Ac00089a031, 1994.
722 Crawford, J. H., Davis, D. D., Chen, G., Buhr, M., Oltmans, S., Weller, R., Mauldin, L.,
723 Eisele, F., Shetter, R., Lefer, B., Arimoto, R., and Hogan, A.: Evidence for
724 photochemical production of ozone at the South Pole surface, Geophysical
725 Research Letters, 28, 3641-3644, Doi 10.1029/2001gl013055, 2001.
726 Dibb, J. E., Talbot, R. W., Munger, J. W., Jacob, D. J., and Fan, S. M.: Air-snow
727 exchange of HNO_3 and NOy at Summit, Greenland, J Geophys Res-Atmos, 103,
728 3475-3486, Doi 10.1029/97jd03132, 1998.
729 Domine, F., and Shepson, P. B.: Air-snow interactions and atmospheric chemistry,
730 Science, 297, 1506-1510, Doi 10.1126/Science.1074610, 2002.
731 Erbland, J., Vicars, W. C., Savarino, J., Morin, S., Frey, M. M., Frosini, D., Vince, E.,
732 and Martins, J. M. F.: Air-snow transfer of nitrate on the East Antarctic Plateau -
733 Part 1: Isotopic evidence for a photolytically driven dynamic equilibrium in
734 summer, Atmos Chem Phys, 13, 6403-6419, DOI 10.5194/acp-13-6403-2013,
735 2013.
736 Erbland, J., Savarino, J., Morin, S., France, J. L., Frey, M. M., and King, M. D.: Air–
737 snow transfer of nitrate on the East Antarctic plateau – Part 2: An isotopic model
738 for the interpretation of deep ice-core records, Atmos. Chem. Phys. Discuss., 15,
739 6887-6966, 10.5194/acpd-15-6887-2015, 2015.
740 France, J. L., King, M. D., Frey, M. M., Erbland, J., Picard, G., Preunkert, S.,
741 MacArthur, A., and Savarino, J.: Snow optical properties at Dome C (Concordia),
742 Antarctica; implications for snow emissions and snow chemistry of reactive

743 nitrogen, Atmos Chem Phys, 11, 9787-9801, DOI 10.5194/acp-11-9787-2011,
744 2011.
745 Frey, M. M., Savarino, J., Morin, S., Erbland, J., and Martins, J. M. F.: Photolysis
746 imprint in the nitrate stable isotope signal in snow and atmosphere of East
747 Antarctica and implications for reactive nitrogen cycling, Atmos Chem Phys, 9,
748 8681-8696, DOI 10.5194/acp-9-8681-2009, 2009.
749 Grannas, A. M., Jones, A. E., Dibb, J., Ammann, M., Anastasio, C., Beine, H. J., Bergin,
750 M., Bottenheim, J., Boxe, C. S., Carver, G., Chen, G., Crawford, J. H., Domine, F., Frey,
751 M. M., Guzman, M. I., Heard, D. E., Helmig, D., Hoffmann, M. R., Honrath, R. E.,
752 Huey, L. G., Hutterli, M., Jacobi, H. W., Klan, P., Lefer, B., McConnell, J., Plane, J.,
753 Sander, R., Savarino, J., Shepson, P. B., Simpson, W. R., Sodeau, J. R., von Glasow,
754 R., Weller, R., Wolff, E. W., and Zhu, T.: An overview of snow photochemistry:
755 evidence, mechanisms and impacts, Atmos Chem Phys, 7, 4329-4373, 2007.
756 Hastings, M. G., Jarvis, J. C., and Steig, E. J.: Anthropogenic Impacts on Nitrogen
757 Isotopes of Ice-Core Nitrate, Science, 324, 1288-1288, Doi
758 10.1126/Science.1170510, 2009.
759 Honrath, R. E., Peterson, M. C., Guo, S., Dibb, J. E., Shepson, P. B., and Campbell, B.:
760 Evidence of NOx production within or upon ice particles in the Greenland
761 snowpack, Geophys Res Lett, 26, 695-698, Doi 10.1029/1999gl900077, 1999.
762 Kaiser, J., Hastings, M. G., Houlton, B. Z., Rockmann, T., and Sigman, D. M.: Triple
763 oxygen isotope analysis of nitrate using the denitrifier method and thermal
764 decomposition of N2O, Analytical Chemistry, 79, 599-607, Doi
765 10.1021/Ac061022s, 2007.

766 Legrand, M. R., and Kirchner, S.: Origins and Variations of Nitrate in South Polar
767 Precipitation, J Geophys Res-Atmos, 95, 3493-3507, Doi
768 10.1029/Jd095id04p03493, 1990.
769 Mack, J., and Bolton, J. R.: Photochemistry of nitrite and nitrate in aqueous
770 solution: a review, J Photoch Photobio A, 128, 1-13, Doi 10.1016/S1010-
771 6030(99)00155-0, 1999.
772 McCabe, J. R., Boxe, C. S., Colussi, A. J., Hoffmann, M. R., and Thiemens, M. H.:
773 dOxygen isotopic fractionation in the photochemistry of nitrate in water and ice,
774 J Geophys Res-Atmos, 110, Artn D15310
775 Doi 10.1029/2004jd005484, 2005.
776 Meusinger, C., Berhanu, T. A., Erbland, J., Savarino, J., and Johnson, M. S.:
777 Laboratory study of nitrate photolysis in Antarctic snow. I. Observed quantum
778 yield, domain of photolysis, and secondary chemistry, J Chem Phys, 140, Doi
779 10.1063/1.4882898, 2014.
780 Michalski, G., Savarino, J., Bohlke, J. K., and Thiemens, M.: Determination of the
781 total oxygen isotopic composition of nitrate and the calibration of a Delta O-17
782 nitrate reference material, Analytical Chemistry, 74, 4989-4993,
783 10.1021/ac0256282, 2002.
784 Miller, C. E.: Photo-induced isotopic fractionation of stratospheric nitrous oxide.,
785 Abstr Pap Am Chem S, 219, U312-U312, 2000.
786 Morin, S., Savarino, J., Frey, M. M., Yan, N., Bekki, S., Bottenheim, J. W., and
787 Martins, J. M. F.: Tracing the Origin and Fate of NO(x) in the Arctic Atmosphere
788 Using Stable Isotopes in Nitrate, Science, 322, 730-732, Doi
789 10.1126/Science.1161910, 2008.

790 Morin, S., Savarino, J., Frey, M. M., Domine, F., Jacobi, H. W., Kaleschke, L., and
791 Martins, J. M. F.: Comprehensive isotopic composition of atmospheric nitrate in
792 the Atlantic Ocean boundary layer from 65 degrees S to 79 degrees N, J Geophys
793 Res-Atmos, 114, Doi: 10.1029/2008jd010696
794 2009.
795 Röthlisberger, R., Hutterli, M. A., Wolff, E. W., Mulvaney, R., Fischer, H., Bigler, M.,
796 Goto-Azuma, K., Hansson, M. E., Ruth, U., Siggaard-Andersen, M. L., and
797 Steffensen, J. P.: Nitrate in Greenland and Antarctic ice cores: a detailed
798 description of post-depositional processes, Ann Glaciol-Ser, 35, 209-216, Doi
799 10.3189/172756402781817220, 2002.
800 Savarino, J., Kaiser, J., Morin, S., Sigman, D. M., and Thiemens, M. H.: Nitrogen and
801 oxygen isotopic constraints on the origin of atmospheric nitrate in coastal
802 Antarctica, Atmospheric Chemistry and Physics, 7, 1925-1945, 2007.
803 Savarino, J., Morin, S., Erbland, J., Grannec, F., Patey, M. D., Vicars, W., Alexander,
804 B., and Achterberg, E. P.: Isotopic composition of atmospheric nitrate in a tropical
805 marine boundary layer, P Natl Acad Sci USA, 110, 17668-17673, DOI
806 10.1073/pnas.1216639110, 2013.
807 Schmidt, J. A., Johnson, M. S., and Schinke, R.: Isotope effects in N2O photolysis
808 from first principles, Atmos. Chem. Phys., 11, 8965-8975, 10.5194/acp-11-8965-
809 2011, 2011.
810 Sigman, D. M., Casciotti, K. L., Andreani, M., Barford, C., Galanter, M., and Bohlke, J.
811 K.: A bacterial method for the nitrogen isotopic analysis of nitrate in seawater
812 and freshwater, Analytical Chemistry, 73, 4145-4153, 2001.
813 Sofen, E. D., Alexander, B., Steig, E. J., Thiemens, M. H., Kunasek, S. A., Amos, H. M.,
814 Schauer, A. J., Hastings, M. G., Bautista, J., Jackson, T. L., Vogel, L. E., McConnell, J.

R., Pasteris, D. R., and Saltzman, E. S.: WAIS Divide ice core suggests sustained changes in the atmospheric formation pathways of sulfate and nitrate since the 19th century in the extratropical Southern Hemisphere, Atmos Chem Phys, 14, 5749-5769, DOI 10.5194/acp-14-5749-2014, 2014.

Vicars, W. C., Morin, S., Savarino, J., Wagner, N. L., Erbland, J., Vince, E., Martins, J. M. F., Lerner, B. M., Quinn, P. K., Coffman, D. J., Williams, E. J., and Brown, S. S.: Spatial and diurnal variability in reactive nitrogen oxide chemistry as reflected in the isotopic composition of atmospheric nitrate: Results from the CalNex 2010 field study, J Geophys Res-Atmos, 118, 10567-10588, Doi 10.1002/Jgrd.50680, 2013.

Werner, R. A., and Brand, W. A.: Referencing strategies and techniques in stable isotope ratio analysis, Rapid Commun Mass Sp, 15, 501-519, Doi 10.1002/Rcm.258, 2001.

Wolff, E. W.: Nitrate in polar ice, Nato Asi Ser Ser I, 30, 195-224, 1995.

Wolff, E. W.: Ice sheets and nitrogen, Philos T R Soc B, 368, Artn 20130127 Doi 10.1098/Rstb.2013.0127, 2013.

Yung, Y. L., and Miller, C. E.: Isotopic fractionation of stratospheric nitrous oxide, Science, 278, 1778-1780, Doi 10.1126/Science.278.5344.1778, 1997.

Zhou, M. Y., Zhang, Z. H., Zhong, S. Y., Lenschow, D., Hsu, H. M., Sun, B., Gao, Z. Q., Li, S. M., Bian, X. D., and Yu, L. J.: Observations of near-surface wind and temperature structures and their variations with topography and latitude in East Antarctica, J Geophys Res-Atmos, 114, Doi 10.1029/2008jd011611, 2009.

Table 1. Sample ID's with their respective sampling dates during the Austral summer 2011/2012 field campaign at Dome C, Antarctica.

Sample ID	Sampling date
UV#0 and control#0	02/12/2011
UV#1 and control#1	10/12/2011
UV#2 and control#2	21/12/2011
UV#3 and control#3	31/12/2011
UV#4 and control#4	10/01/2012
UV#5 and control#5	20/01/2012
UV#6 and control#6	30/01/2012

Table 2. The apparent nitrogen isotopic fractionations determined for both pits excluding all the samples between 0-7 cm or using the δ^{15}N signal to identify if influenced by external processes. The correlation coefficients (r^2) and significance (p) are also given for the derived $^{15}\varepsilon_{app}$ values derived using the δ^{15}N signal. Note that due to insignificant change in nitrate mass and isotopic composition, the linear fits for samples #0 and #1 from both pits were only weakly correlated, and are not given in table 2.

Sampling No.	$^{15}\varepsilon_{app}$ (± 1-σ)/ ‰ (Removing all samples at 0-7 cm depth)	$^{15}\varepsilon_{app}$ (± 1-σ)/ ‰ (Using the δ^{15}N signal to exclude some points in the UV-pit samples)	r^2	p
UV#2	-18.0 ± 7.3	-72.7 ± 9.7	0.903	0.000292
UV#3	-25.7 ± 13.8	-57.2 ± 27.9	0.456	0.015800
UV#4	-47.8 ± 10.0	-72.3 ± 12.9	0.762	0.000208
UV#5	-48.6 ± 18.9	-65.8 ± 5.0	0.529	0.007300
UV#6	-58 -58.3 ± 20.0	-69.0 ± 11.8	0.792	0.000243
Control#2	-12.9 ± 1.9	-12.9 ± 9.7	0.797	0.000010
Control#3	-7.4 ± 2.3	-7.4 ± 2.3	0.443	0.006760
Control#4	-12.9 ± 2.4	-17.7 ± 28.1	0.646	0.029300
Control#5	-13.2 ± 1.1	-13.9 ± 1.7	0.884	0.000002
Control#6	-15.0 ± 0.9	-13.8 ± 2.4	0.767	0.000086

Table 3. Apparent isotopic fractionations ($^{15}\varepsilon_{app}$) observed in previous studies compared to the results obtained here.

	$^{15}\varepsilon$/ ‰	Reference
$^{15}\varepsilon_{app}$/‰	-53.9 ± 9.7	Blunier et al 2005[a]
	-50.0 ± 10.0 (DC 04)	Frey et al 2009[a]
	-71.0 ± 12.0 (DC 09)	Frey et al 2009[a]
	-59.0 ± 10.0	Erbland et al 2013[b]
	-67.8 ± 12.0	This study[c]
$^{15}\varepsilon_{photo}$/‰	-48.0	Frey et al 2009[d]
	-47.9 ± 6.8	Berhanu et al 2014[e]

[a]*Values determined for Dome C*

[b]*An apparent average value derived for different locations on the East Antarctic Plateau*

[c]*The* $^{15}\varepsilon$ *determined for the UV samples in this study*

[d]*Determined using the ZPE shift model and using the solar actinic flux of Dome C derived from snow TUV model*

[e]*A laboratory result observed using snow from Dome C and a Xe lamp with a UV-filter at 320 nm (relevant to Dome C conditions) (Berhanu et al.2014)*

Table 4. Compiled $^{18}\varepsilon$ and ^{17}E values obtained from this study for the UV samples and previous studies

$^{18}\varepsilon_{UV}$(± 1-σ)/ ‰	$^{17}E_{UV}$(± 1-σ)/ ‰	Reference
6.0 ± 3.0 (DC 04)	1.0 ± 0.2	Frey et al 2009[a]
9.0 ± 2.0 (DC 09)	2.0 ± 0.6	Frey et al 2009[a]
8.7 ± 2.4	2.0 ± 1.0	Erbland et al 2013[b]
12.5 ± 6.7	2.2 ± 1.4	This study[c]

[a]*Determined by Frey et al. (2009) at Dome C during the summer campaigns in 2004 and 2007*

[b]*An average value determined by Erbland et al.(2013) for the Eastern Antarctic Plateau*

[c]*An average value determined by this study for all the UV samples*

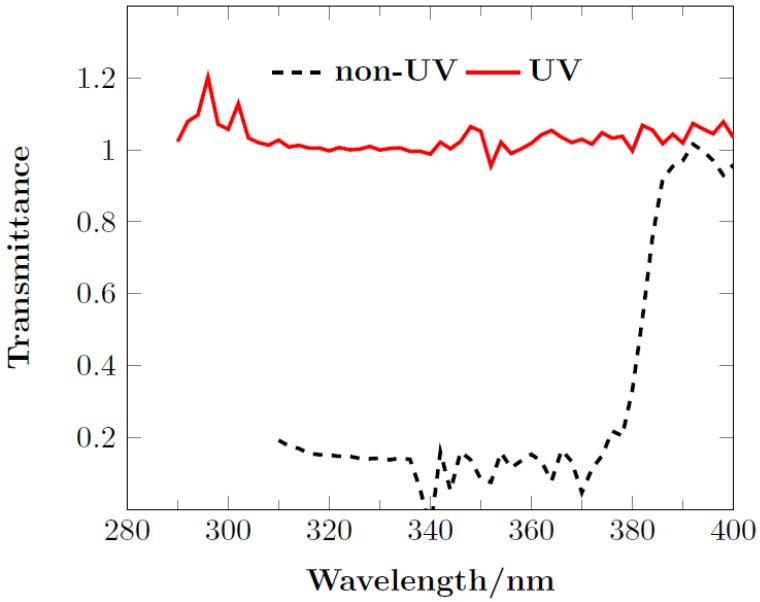

Figure 1. *Transmittance as measured for the control and the UV plates. The UV plate transmits solar UV above 290 nm, whereas the control plate has a cut off at ca. 375 nm (note that the control plate has an average transmittance of 15 % below 375 nm). As transmission was measured as the ratio between solar light below plexi-plate to light above the plexi-plate, light reflected back by the snow might lead to transmittance greater than one.*

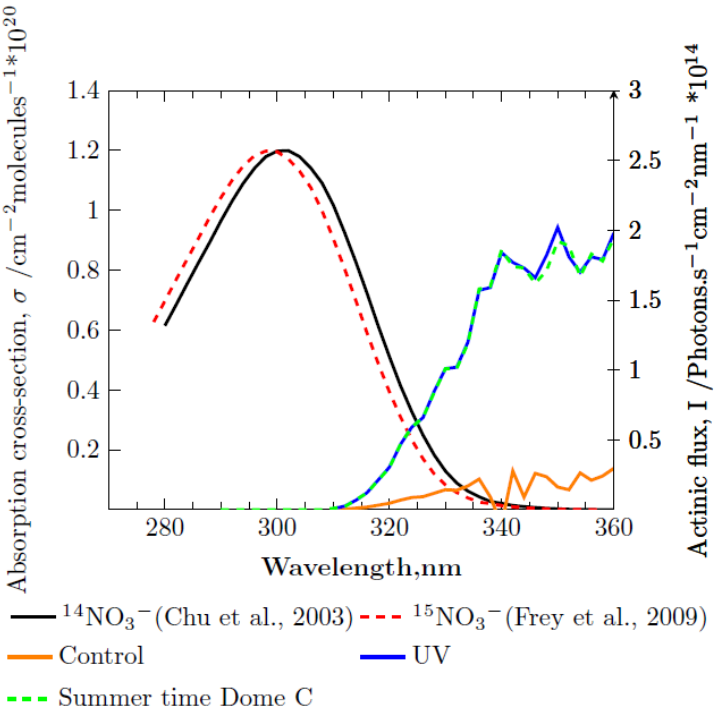

Figure 2. *The absorption cross-section of $^{14}NO_3^-$ measured in the liquid phase and the absorption cross-section of $^{15}NO_3^-$ determined using the ZPE shift model (left y-axis). The absorption cross section of $^{15}NO_3^-$ was derived by applying an average shift of 0.5 nm on $^{14}NO_3^-$. The 2 nm shift has been manually emphasized (note that in reality the two curves nearly overlap). Plotted on the right y-axis is the solar spectrum derived using the TUV model at Dome C conditions (ozone column depth of 297 DU and an albedo of 0.9) and expected UV fluxes in the presence of the plexi-plate filters.*

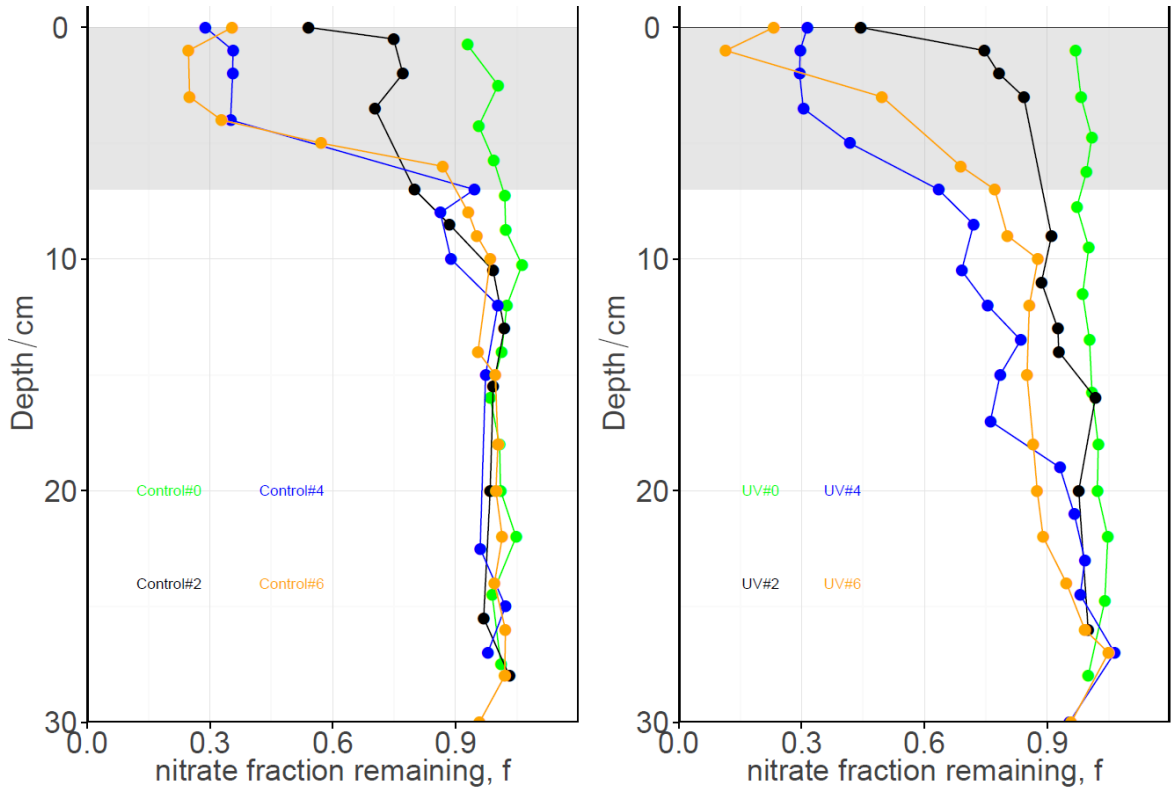

Figure 3. *Plot of the nitrate fraction remaining in the snow (f) with depth. Control samples (reduced solar UV) are plotted in the left panel and UV-exposed samples are plotted in the right panel. The numbers denote the sampling events, which were carried out at 10-day intervals from 02/12/2011 to 30/01/12. The grey shaded region shows the depth where external factors (mainly mixing) play a significant role.*

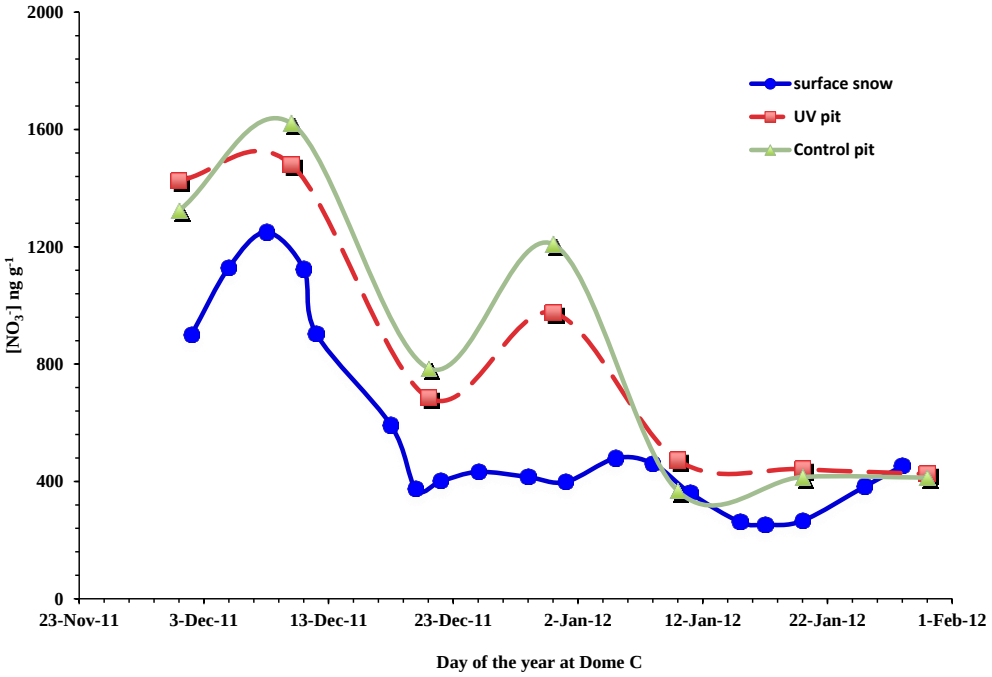

Figure 4. *The nitrate concentration profile for the surface snow collected in the vicinity of the two pits compared with the UV and control pit surface snow (0 – 2 cm depth).*

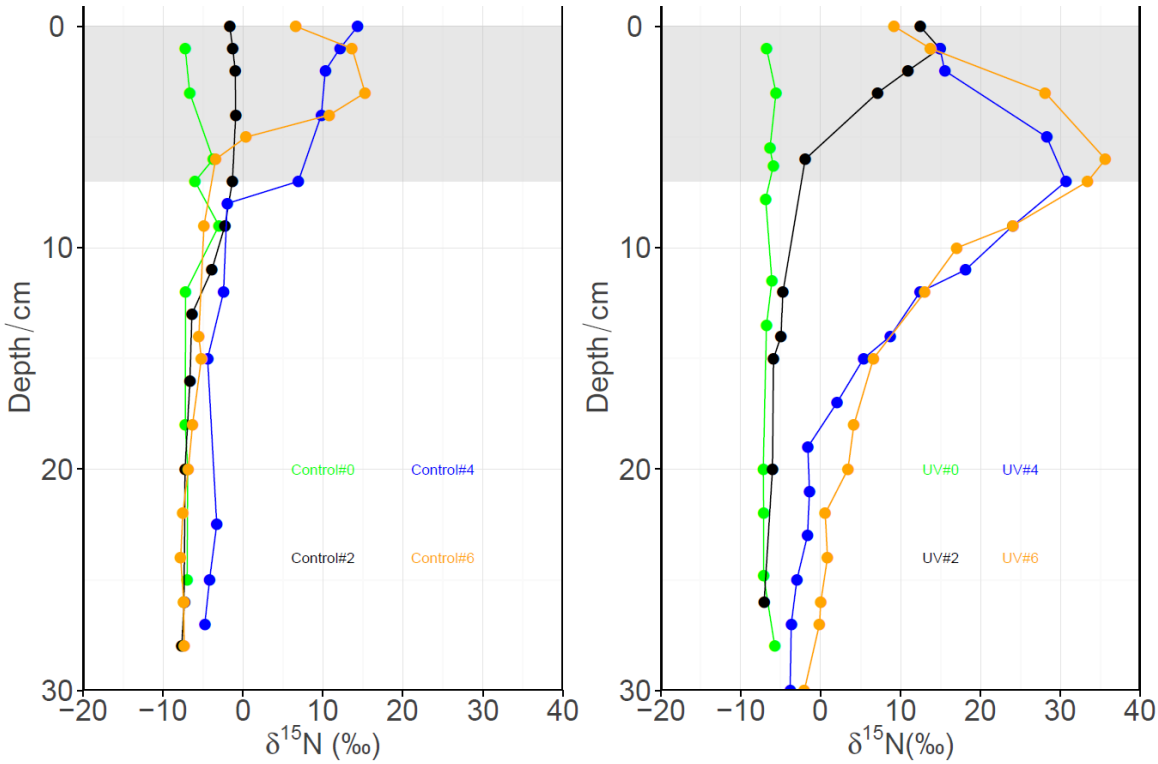

Figure 5. *$\delta^{15}N$ depth profiles for snow nitrate in the control (top panel)and UV (bottom panel) pits.*

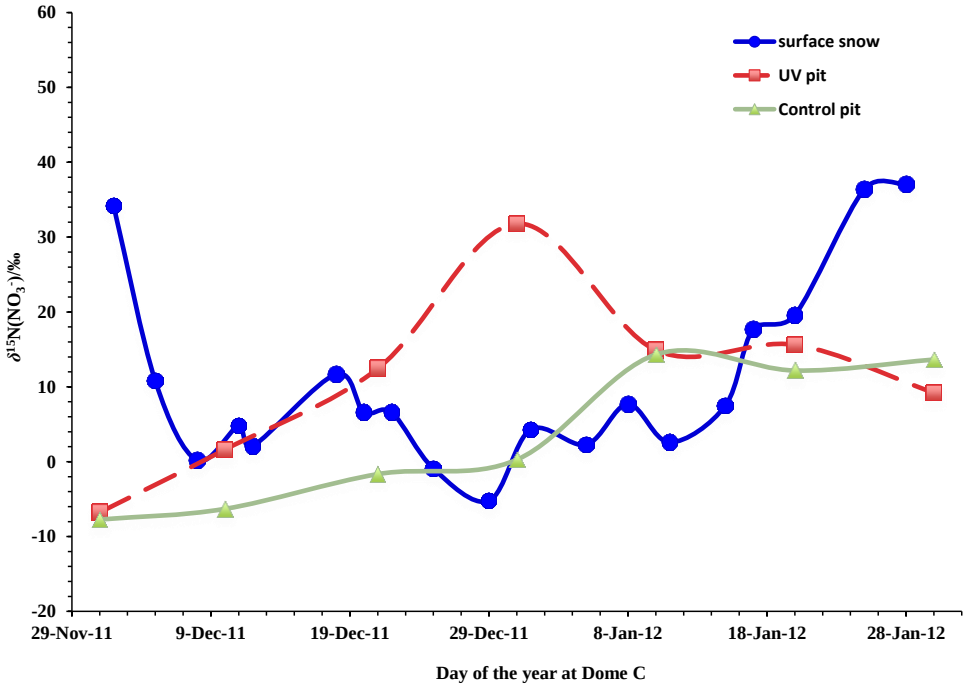

Figure 6. *$\delta^{15}N$ time-series for nitrate in natural surface snow compared to surface snow sampled from the UV and control pits.*

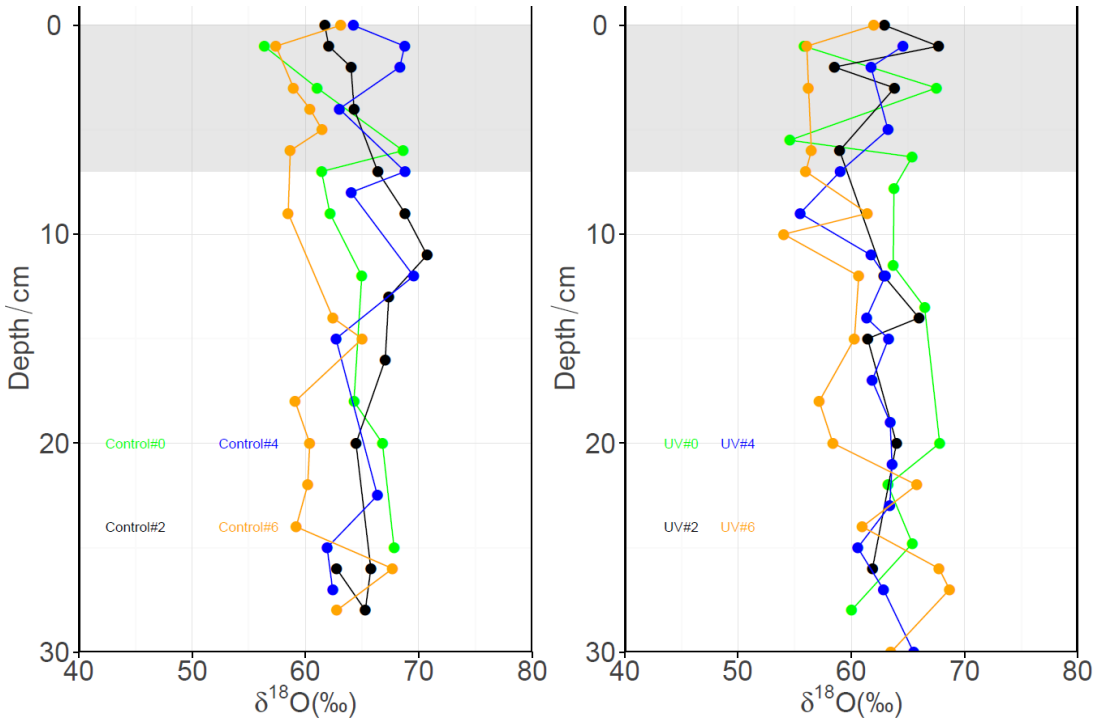

Figure 7. *$\delta^{18}O$ depth profiles for snow nitrate in the control (left panel) and UV (right panel) pits.*

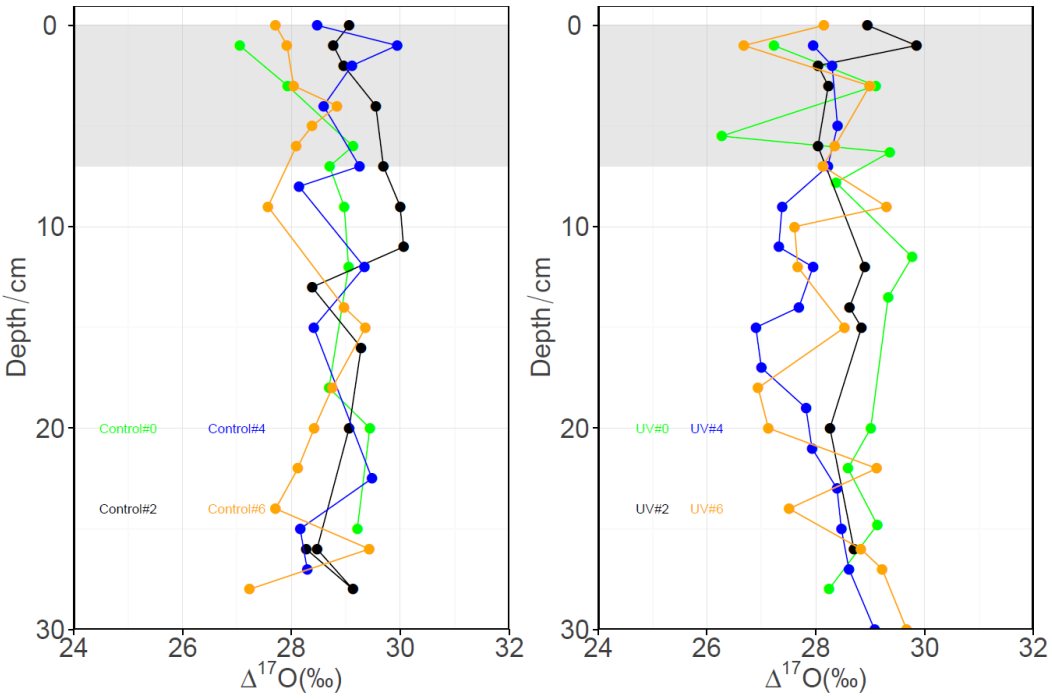

Figure 8. *Same as Figure 7 but for* $\Delta^{17}O$

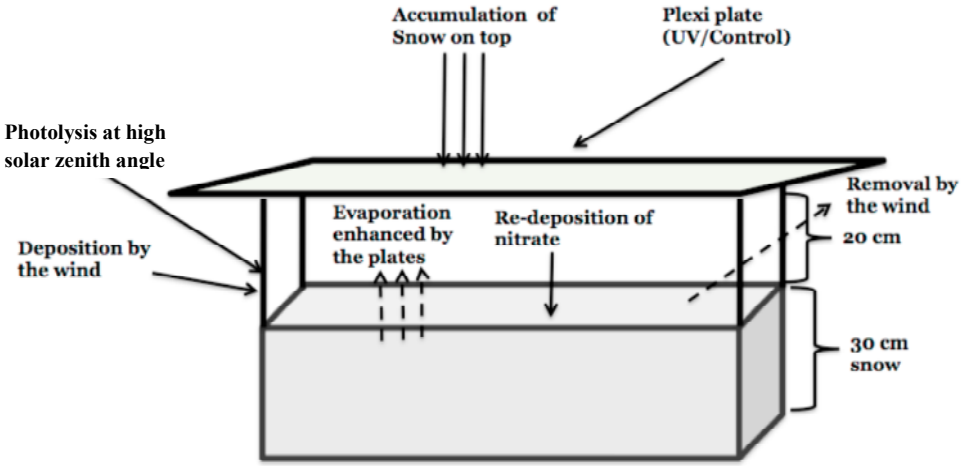

Figure 9. *Schematic showing the possible external processes that could affect the surface layers of both the UV and control pits. These include evaporation, wind deposition/removal, and photolysis at high solar zenith angle.*

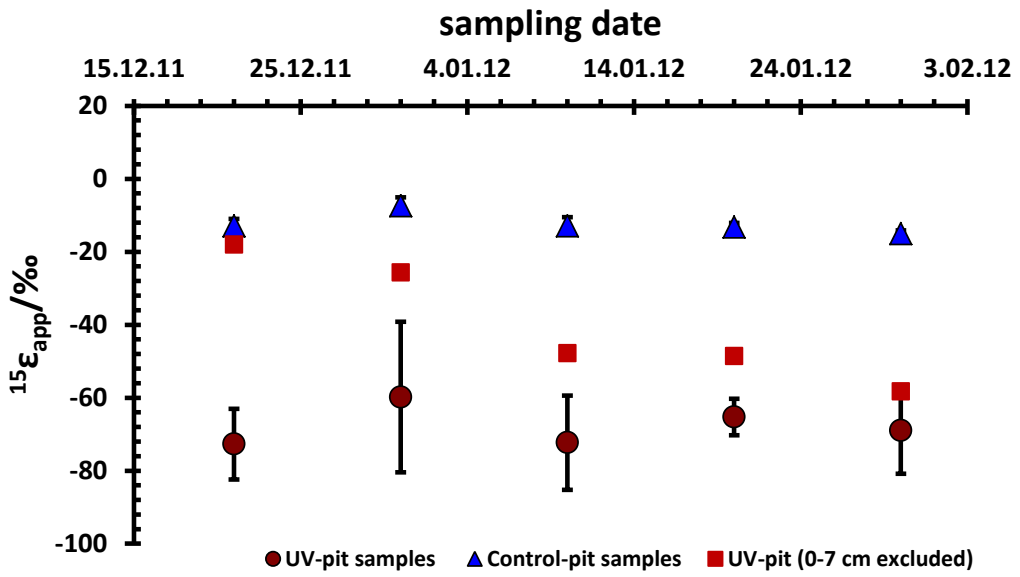

Figure 10. *$^{15}\varepsilon_{app}$ values determined for the control samples (triangles), UV samples excluding all samples between 0-7 cm (squares), and the UV samples obtained using the $\delta^{15}N$ signal to identify data points affected by non-photolytic processes (circles) rather than by excluding all 0-7 cm data. Note that excluding the entire top 7 cm data introduced an apparent trend where $^{15}\varepsilon_{app}$ decreases with time. Errors are determined by the least square fit method as in Frey et al. (2009).*

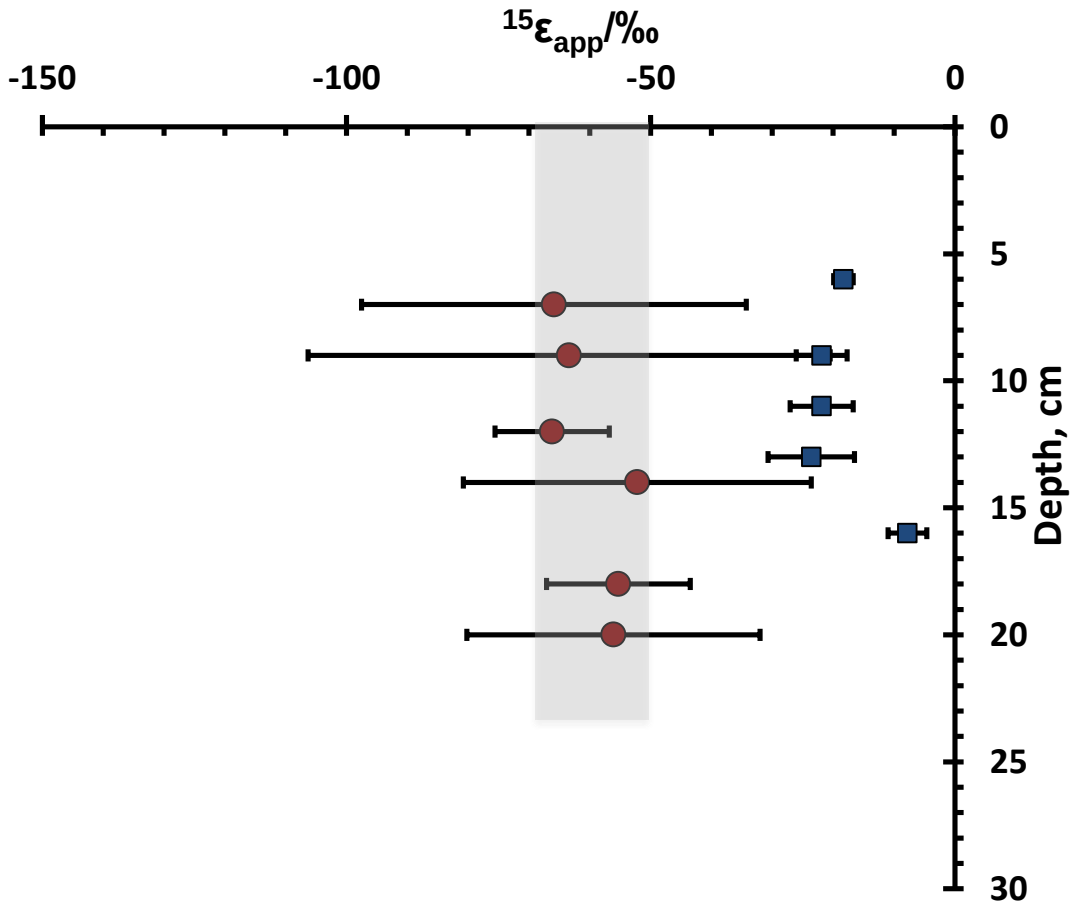

Figure 11. *The depth profile of $^{15}\varepsilon$ for the UV pit. The $^{15}\varepsilon$ was calculated from samples collected at the same depth during each sampling event. Error bars are calculated using the least square fit method as in Frey et al. (2009). The shaded region represents the measured $^{15}\varepsilon$ range of -50 ‰ to -70 ‰.*